Space-Time Coding with Multilevel Protection for Multimedia Transmission in MIMO Systems

Jian-Jia Weng, Chung-Hsuan Wang, and Li-Der Jeng†
Department of Communications Engineering, National Chiao Tung University, Hsinchu, Taiwan 30010, R.O.C.
†Department of Electronic Engineering, National Chung Yuan Christian University, Chung Li, Taiwan 32023, R.O.C.
chaselweng.cm95g@nctu.edu.tw, chwang@mail.nctu.edu.tw, lider@cycu.edu.tw

***Abstract*—In this paper, space-time coding schemes with full transmit diversity are investigated for unequal error protection (UEP). Effective performance indicies are proposed to measure the intrinsic UEP capability of space-time codes, based on which we demonstrate that space-time trellis codes and super-orthogonal space-time trellis codes can be used for UEP as long as the corresponding encoders are properly designed. In addition, UEP convolutional codes are concatenated with space-time block codes to construct another full-diversity UEP scheme which can provide more choices of UEP levels. Finally, good UEP codes are given by a computer search.**

I. Introduction

In many applications, e.g., broadcast systems and visual/speech communication systems, the source data are of unequal error sensitivities or face different levels of noise corruption. To make the best use of the channel bandwidth in those systems, it is desirable to design an error-correcting code with the capability of unequal error protection (UEP) which can provide different levels of protection against errors. However, literatures about UEP were focused on channel codes without transmitter diversity [1]-[6]. Although good UEP codes have been provided, they inevitably demand the undesired bandwidth expansion. Space-time coding not only inherits the high data rate transmission of multiple-input and multiple-output (MIMO) systems but also provides excellent performance against multipath fading [7]-[8]. Nevertheless, only a few of studies are about space-time coding for UEP. Among those, the UEP capability of space-time codes was observed in terms of the different diversity orders embedded for distinct messages [9]; the authors also presented a construction of two-level UEP codes of short block length. Another diversity-based UEP scheme based on the layered space-time architecture was proposed for multimedia transmission in [10]. In [11][12], space-time trellis codes are incorporated with puncturing to construct a powerful UEP scheme with flexible choices of rates and UEP levels.

In this paper, the intrinsic UEP capability of space-time codes is investigated. Firstly, two types of performance indicies: the effective rank & determinant for the low-diversity case and the effective distance for the high-diversity case are proposed for space-time codes. Based on the proposed UEP measurements, we observe that different input streams of the space-time trellis codes (STTC) may experience different levels of protection; STTC encoders with the special architecture in [7] can thus be used for UEP as long as the associated generator sequences are properly designed. We also demonstrate that super-orthogonal space-time trellis codes (SOSTTC) [13] originally designed for full-diversity and high-rate transmission can provide the desired UEP capability. In addition, conventional UEP convolutional codes (CC) are concatenated with space-time block codes (STBC) to construct another full-diversity UEP scheme; compared with the UEP-STTC and UEP-SOSTTC, this scheme can provide larger performance gaps between UEP levels. Furthermore, good UEP codes based on the above space-time coding schemes with different UEP levels, bandwidth efficiencies, and memories are provided by a computer search. Finally, an example of multimedia transmission is given to visualize the benefits of the proposed UEP schemes.

The rest of this paper is organized as follows. In Section II, the UEP capability of space-time codes is investigated together with the effective measurements. The UEP schemes based on STTC, SOSTTC, and UEPCC-STBC are described in Section III. In Section IV, simulation results are provided for performance verification. Finally, a summary is drawn in Section V to conclude this work.

II. UEP Capability of Space-Time Codes and the Effective Measurements

Consider a space-time code with N_T transmit antennas and N_R receive antennas. Let $\boldsymbol{G}$ be the corresponding encoder which maps K streams of input information into coded sequences for transmission. Denote by $u_{i,t}$ and $x_{j,t}$ the message fed to the ith input of encoder and the modulated symbol transmitted by the jth antenna at time t, respectively, $\forall$ $1 \le i \le K$ and $1 \le j \le N_T$. For a data frame of length-L, let $U_i = (u_{i,1}, u_{i,2}, \cdots, u_{i,L})$ be the information sequence fed to the ith input of $\boldsymbol{G}$ and $U = (U_1^T, U_2^T, \cdots, U_K^T)^T$ be the information matrix for encoding, where T denotes the operation of taking transpose. The codeword matrix X for transmission is defined by

$$\begin{pmatrix} x_{1,1} & x_{1,2} & \cdots & x_{1,L} \\ x_{2,1} & x_{2,2} & \cdots & x_{2,L} \\ \vdots & \vdots & \ddots & \vdots \\ x_{N_T,1} & x_{N_T,2} & \cdots & x_{N_T,L} \end{pmatrix}$$

where the (j,t)th entry indicates the data transmitted by the jth antenna at time t.

In conventional, space-time codes are used for equal error protection; in such applications, the diversity order defined as the minimum rank of the codeword distance matrix is unarguably an effective parameter for performance evaluation [7]. However, space-time codes with the encoders of multiple

978-1-4244-5213-4/09/ $26.00 ©2009 IEEE

inputs may possess the UEP capability. For example, consider a space-time trellis code with generator sequences:

$$g_1 = [(0,1),(1,0)],\ g_2 = [(2,2),(0,2)] \tag{1}$$

which is equipped with the quaternary phase-shift keying (QPSK) modulation of symbol energy E_s for transmission over a Rayleigh fading channel with the additive white Gaussian noise of two-sided power spectral density $N_0/2$. For binary inputs $(u_{1,t}, u_{2,t})$, the corresponding encoder outputs $(v_{1,t}, v_{2,t})$ are obtained by

$$(v_{1,t},v_{2,t}) = u_{1,t}(0,1) \oplus_4 u_{1,t-1}(1,0) \oplus_4 u_{2,t}(2,0) \oplus_4 u_{2,t-1}(2,2)$$

where $\oplus_4$ stands for the modulo 4 addition; $v_{1,t}$ and $v_{2,t}$ are then mapped to the following modulated symbols for transmission:

$$x_{i,t} = \sqrt{E_s}\exp(\sqrt{-1}\cdot v_{i,t}\cdot \pi/2) \quad \text{for } i = 1 \text{ and } 2.$$

Suppose the receiver is equipped with 4 antennas. Observed from the performance plots in Fig. 1, $u_{1,t}$'s and $u_{2,t}$'s both experience the same diversity order (since the corresponding BER curves have the same slope asymptotically) but $u_{2,t}$'s receive a better protection than $u_{1,t}$'s with a coding gain about 2 dB at BER 10^{-5}. This code can hence be used for two-level UEP as long as the data of distinct BER requirements are properly fed into the encoder. In addition, the embedded diversity order originally addressed in [9] to characterize the UEP capability seems unable to reflect the UEP behavior in this case. Besides the diversity order, new measurements to provide a more precise evaluation of the UEP capability of space-time codes are described below.

To evaluate the BER of the lth input-stream of $\boldsymbol{G}$ for some $l \in \{1, 2, \cdots, K\}$, consider two codeword matrices X and $\hat{X}$ with $U_l \neq \hat{U}_l$. Define the codeword distance matrix $A(X, \hat{X})$ between X and $\hat{X}$ by

$$A(X,\hat{X}) = (X-\hat{X})\cdot(X-\hat{X})^H$$

where H stands for the operation of taking Hermitian. Denote by $r(X, \hat{X})$ and $\{\lambda_i(X, \hat{X}),\ \forall\ 1 \le i \le N_T\}$ the rank and eigenvalues of $A(X, \hat{X})$, respectively. Assume $\lambda_i(X, \hat{X}) \ge \lambda_{i+1}(X, \hat{X})$, $\forall\ i$, without loss of generality. For Rayleigh fading channels, the pairwise error probability that the maximum likelihood decoder decides in favor of $\hat{X}$ than X to make an error decision on the lth input-stream can be upper bounded by

$$\left(\prod_{i=1}^{r(X,\hat{X})}\frac{\lambda_i(X,\hat{X})}{E_s}\right)^{-N_R}\left(\frac{E_s}{4N_0}\right)^{-r(X,\hat{X})N_R} \tag{2}$$

at high signal-to-noise ratios (SNR), based on the analysis of codeword error probability for ordinary space-time codes in [7]. For the case of $r(X, \hat{X})N_R \ge 4$, the upper bound of the pairwise error probability can be further expressed as

$$\frac{1}{4}\exp\left(-\frac{N_R}{4}\cdot\frac{E_s}{N_0}\cdot\sum_{i=1}^{N_T}\lambda_i(X,\hat{X})\right) \tag{3}$$

with a better approximation than (2) by generalizing the derivation in [8]. Let $r_{\min,l}(\boldsymbol{G})$ denote the minimum effective rank associated with the lth input of $\boldsymbol{G}$ which is defined as

$$\min_{\{\forall X\neq\hat{X}\in\boldsymbol{C}|U_l\neq\hat{U}_l\}} r(X,\hat{X}).$$

According to the value of $r_{\min,l}(\boldsymbol{G})N_R$, i.e., the effective diversity gain for the lth input sequence, two types of UEP measurement are given as follows.

A. The Low-Diversity Case: $r_{\min,l}(\boldsymbol{G})N_R < 4$

Define the minimum effective determinant associated with the lth input of $\boldsymbol{G}$ by

$$\det_{\min,l}(\boldsymbol{G}) = \min_{\{\forall X\neq\hat{X}\in\boldsymbol{C}|U_l\neq\hat{U}_l\}}\ \prod_{i=1}^{r_{\min,l}(\boldsymbol{G})}\frac{\lambda_i(X,\hat{X})}{E_s}.$$

By (2), the BER of the lth input-stream of $\boldsymbol{G}$, denoted by $P_l(\boldsymbol{G})$, can be dominated by the following term:

$$\det_{\min,l}(\boldsymbol{G})^{-N_R}\cdot\left(\frac{E_s}{4N_0}\right)^{-r_{\min,l}(\boldsymbol{G})N_R}$$

at high SNRs. Large values of $r_{\min,l}(\boldsymbol{G})$ and $\det_{\min,l}(\boldsymbol{G})$ can thus imply a small $P_l(\boldsymbol{G})$.

B. The High-Diversity Case: $r_{\min,l}(\boldsymbol{G})N_R \ge 4$

Let $d^2(X, \hat{X})$ be the effective distance between X and $\hat{X}$ defined by

$$\sum_{t=1}^{L}\sum_{j=1}^{N_T}|x_{j,t}-\hat{x}_{j,t}|^2$$

and denote by $d^2_{\min,l}(\boldsymbol{G})$ the minimum effective distance corresponding to the lth input of $\boldsymbol{G}$, i.e.,

$$d^2_{\min,l}(\boldsymbol{G}) = \min_{\{\forall X\neq\hat{X}\in\boldsymbol{C}|U_l\neq\hat{U}_l\}} d^2(X,\hat{X}).$$

Based on the observation that

$$\sum_{i=1}^{N_T}\lambda_i(X,\hat{X}) = \sum_{t=1}^{L}\sum_{j=1}^{N_T}|x_{j,t}-\hat{x}_{j,t}|^2$$

a large value of $d^2_{\min,l}(\boldsymbol{G})$ then implies a better BER for the lth input-stream of $\boldsymbol{G}$, since $P_l(\boldsymbol{G})$ is now dominated by

$$\exp\left(-\frac{N_R}{4}\cdot\frac{E_s}{N_0}\cdot d^2_{\min,l}(\boldsymbol{G})\right)$$

at high SNRs by (3).

Define the effective rank vector $R(\boldsymbol{G})$, the effective determinant vector $\Delta(\boldsymbol{G})$, and the effective distance vector $\Omega(\boldsymbol{G})$ of $\boldsymbol{G}$ by

$$\begin{aligned} R(\boldsymbol{G}) &= (r_{\min,1}(\boldsymbol{G}), r_{\min,2}(\boldsymbol{G}), \cdots, r_{\min,K}(\boldsymbol{G})) \\ \Delta(\boldsymbol{G}) &= (\det_{\min,1}(\boldsymbol{G}), \det_{\min,2}(\boldsymbol{G}), \cdots, \det_{\min,K}(\boldsymbol{G})) \\ \Omega(\boldsymbol{G}) &= \left(d^2_{\min,1}(\boldsymbol{G}), d^2_{\min,2}(\boldsymbol{G}), \cdots, d^2_{\min,K}(\boldsymbol{G})\right). \end{aligned} \tag{4}$$

The UEP capability of $\boldsymbol{G}$ can then be characterized by $(R(\boldsymbol{G}),\ \Delta(\boldsymbol{G}))$ for the low-diversity case and $\Omega(\boldsymbol{G})$ for the high-diversity case, respectively. In general, the larger $(R(\boldsymbol{G}),\ \Delta(\boldsymbol{G}))$ or $\Omega(\boldsymbol{G})$ is, the better the UEP capability is; the number of distinct components in $R(\boldsymbol{G})$, $\Delta(\boldsymbol{G})$, $\Omega(\boldsymbol{G})$ also corresponds to the available levels for UEP. Recall the space-time encoder of generator sequences in (1); in this case, $K = 2$, $N_T = 2$, and $N_R = 4$. By (4), we have

$R(\boldsymbol{G}) = (2,2)$, $\Delta(\boldsymbol{G}) = (4,4)$, and $\Omega(\boldsymbol{G}) = (4,12)$. Since $r_{\min,l}(\boldsymbol{G})N_R \geq 4$ for l=1,2, the unequal effective distances in $\Omega(\boldsymbol{G})$ thus successfully reflect the two-level UEP for $u_{1,t}$'s and $u_{2,t}$'s revealed in Fig. 1.

III. Full-Diversity UEP Schemes Based on STTC, SOSTTC, and UEPCC-STBC

In conventional approaches [9][10], different diversity orders were designed for distinct messages to achieve UEP. The consequent UEP schemes thus can not obtain full transmit diversity and suffer from a poor performance of average BER. However, we observe that some space-time architectures with full diversity are inherently with the UEP capability in terms of the proposed effective measurements, although such a desirable capability is totally ignored by the previous researches. Designs based on those architectures can then accomplish UEP without any loss of transmit diversity. In the following, we first demonstrate the feasibility of STTC and SOSTTC for UEP. A concatenation of UEPCC and STBC which can assure full diversity and provide more choices of UEP levels is presented as well.

A. STTC for UEP

STTC with the special encoder architecture in [7], for which total memory elements are uniformly distributed in the shift-registers for all input streams, have been shown to achieve full-diversity transmission and provide excellent performance against multipath fading [7][8]. Conventional designs of STTC are focused on maximizing the average diversity and coding gains of the space-time coded system. Therefore, most of the optimal codes constructed previously, no matter for the low-diversity or high-diversity cases, can provide only a single level of protection. For example, consider an optimal code $\hat{\boldsymbol{C}}$ obtained for the high-diversity case with the encoder $\hat{\boldsymbol{G}}$ of generator sequences [8]

$$\hat{g}_1 = [(0,2),(2,0)] \quad \text{and} \quad \hat{g}_2 = [(0,1),(1,0)] \tag{5}$$

which is equipped with the QPSK modulation; in this case, K = 2 and N_T = 2. By the definitions in Section II, we have $R(\hat{\boldsymbol{G}})$ = ($r_{\min,1}(\hat{\boldsymbol{G}})$, $r_{\min,2}(\hat{\boldsymbol{G}})$) = (2,2) and $\Omega(\hat{\boldsymbol{G}})$ = ($d^2_{\min,1}(\hat{\boldsymbol{G}})$, $d^2_{\min,2}(\hat{\boldsymbol{G}})$) = (4,4). $\hat{\boldsymbol{C}}$ achieves the full diversity as expected since $r_{\min,1}(\hat{\boldsymbol{G}}) = r_{\min,2}(\hat{\boldsymbol{G}}) = N_T$. However, the observation of $d^2_{\min,1}(\hat{\boldsymbol{G}})$ = $d^2_{\min,2}(\hat{\boldsymbol{G}})$ implies that only a single level of protection is available although K = 2.

To provide UEP by STTC, we still employ the same encoder architecture to guarantee full transmit diversity but the corresponding generator sequences are now searched according to the proposed UEP measurements, instead of the average diversity and coding gains. For the low diversity case, an optimum choice of the generator sequences should result in ($R(\boldsymbol{G})$, $\Delta(\boldsymbol{G})$) as large as possible. The generator sequences are then optimized to maximize $\Omega(\boldsymbol{G})$ for the high diversity case. By an exhaustive computer search, families of full-diversity STTC with good UEP capability for both of the low-diversity and high-diversity cases have been obtained; only the family with two transmit antennas and QPSK are given in Table I for illustration due to the length limitation. Note that, compared with the optimal codes with the same rates and memories in [7], UEP codes obtained for the low-diversity case have the same or larger ($R(\boldsymbol{G})$, $\Delta(\boldsymbol{G})$)'s; the new constructed UEP codes can hence provide better protection for all input streams.

B. SOSTTC for UEP

SOSTTC were first introduced in [13] to take the advantages of STBC and STTC. By employing the trellis structure similar to STTC but choosing a set of parameterized class of STBC as the space-time signal points for transmission, SOSTTC have been verified to provide a good trade-off between the rate and diversity of space-time coded systems. Conventional designs on SOSTTC are focused on maximizing the minimun coding gain distance [13] of all codeword matrices only; the intrinsic UEP capability of SOSTTC is thereby neglected unwittingly. However, we observe that SOSTTC can be used for UEP as long as the codes are now designed by optimizing the proposed effective measurements rather than the original performance index. Consider an example of SOSTTC with K=4, N_T=2, and the QPSK modulation which chooses the following two types of STBC for transmission:

$$\text{Type1 STBC: } \begin{pmatrix} s_1 & s_2 \\ -s_2^* & s_1^* \end{pmatrix}, \ \text{Type2 STBC: } \begin{pmatrix} -s_1 & s_2 \\ s_2^* & s_1^* \end{pmatrix}$$

where s_1 and s_2 are mapped from the input vector ($u_{1,t}$, $u_{2,t}$, $u_{3,t}$, $u_{4,t}$) by the encoder $\boldsymbol{G}$ as depicted in Fig. 2, where the associated trellis module has two states and at each time instant the type of STBC used for transmission is determined by the value of current state. By the definitions in Section II, we have $R(\boldsymbol{G}) = (2,2,2,2)$, $\Delta(\boldsymbol{G}) = (4,16,16,64)$, and $\Omega(\boldsymbol{G}) = (4,8,8,16)$. This full-diversity code can thus provide three-level UEP for both of the low-diversity and high-diversity cases since the components in $\Delta(\boldsymbol{G})$ and $\Omega(\boldsymbol{G})$ are now of three distinct values respectively.

C. UEP Scheme Based on UEPCC-STBC

STBC with the orthogonal design have been verified to achieve full transmit diversity but with the drawback of no coding gain [14]. On the other hand, UEP convolutional codes, originally designed for the system of single transmit antenna, can provide rich of coding gain for different input streams, but the direct use of them in fading channels usually suffers from a performance degradation. To take both of the advantages of STBC and UEPCC, a space-time UEP scheme which concatenates the both schemes as indicated in Fig. 3 is proposed here. In this concatenated scheme, the information bits are first encoded by an (N,K,V) UEP convolutional code with proper UEP capability to attain the desirable coding gain, whose encoder has K inputs, N outputs, and memory V. Let $(c_{1,t},\cdots,c_{N,t})$ denote the vector of coded bits at time t. $(c_{1,t},\cdots,c_{N,t})$ is then processed by a specially designed $N_s \times N$ mapping matrix Q to generate N_s modulated symbols $(y_{1,t},\cdots,y_{N_s,t})$ by

$$(y_{1,t},\cdots,y_{N_s,t})^T = Q \cdot (c_{1,t},\cdots,c_{N,t})^T.$$

Finally, $(y_{1,t},\cdots,y_{N_s,t})$ is transformed into a space-time codeword matrix with N_T transmit antennas by a STBC encoder to achieve the full transmit diversity. By an exhaustive computer search, families of full-diversity codes with good

UEP capability for both of the low-diversity and high-diversity cases have been obtained. Only the family with two transmit antennas and the Alamouti STBC [14] with QPSK are given in Table II, where the generator matrices of UEPCC are chosen to be canonical to avoid the catastrophic encoders and the corresponding entries are expressed in octal form, for illustration due to the length limitation.

IV. Simulation Results

To verify the validity of the proposed UEP measurements, UEP schemes based on STTC, SOSTTC, and UEPCC-STBC are simulated for transmission over a block fading channel, for which the fading gain is assumed to be constant within each data frame of 130 symbols. In Fig. 1, the BER curves corresponding to different input streams of the high-diversity STTC are plotted. From the simulation results, all curves are observed to have the same slope asymptotically; the code in Table I achieves two-level UEP but the optimal code by the conventional design can provide only a single level of protection. Compared with the observation that $R(\boldsymbol{G})$ = $R(\hat{\boldsymbol{G}})$ = (2,2), $\Omega(\boldsymbol{G}) = (4, 12)$, and $\Omega(\hat{\boldsymbol{G}})$ = (4,4), the proposed measurements can successfully predict the UEP capability. Performance plots of the SOSTTC illustrated in Section III-B are shown in Fig. 4; the three-level UEP observed in Fig. 4 is also consistent with the prediction of $\Delta(\boldsymbol{G}) = (4, 16, 16, 64)$ for the low-diversity case. In addition, consider the UEP scheme based on the (4,2,2) UEP convolutional code in Table II with $\Delta(\boldsymbol{G}) = (4, 144)$ and $\Omega(\boldsymbol{G}) = (4, 24)$. Observed from Fig. 5, the proposed measurements can precisely reflect the UEP behavior for the both cases of N_R = 2 and 4. Owing to the different coding gains introduced by the UEP convolutional code, this scheme can provide apparent performance gaps (up to 6dB SNR gain at BER 10^{-5}) between two UEP levels.

To demonstrate the benefit of applying UEP, a gray image is transmitted over Rayleigh fading channels under the protection of the both STTCs with the same rate and memory considered in Fig. 1. At SNR = -1dB, the reconstructed images with and without applying UEP are shown in Fig. 6(a) and Fig. 6(b). It can be seen that the better visual quality is obtained with the usage of UEP. The peak signal-to-noise ratio (PSNR) curves in Fig. 7 also shows the improvement of the reconstructed images with the aid of UEP.

V. Conclusion

In this paper, two types of performance indicies: ($R(\boldsymbol{G})$, $\Delta(\boldsymbol{G})$) and $\Omega(\boldsymbol{G})$ are proposed to measure the intrinsic UEP capability of space-time codes. Based on those measurements, we demonstrate that STTC and SOSTTC can be used for UEP as long as the corresponding encoders are properly designed. In addition, UEPCC are concatenated with STBC to construct another full-diversity UEP scheme which can provide more choices of UEP levels. Simulation results also verify the effectiveness of the proposed UEP measurements for multimedia transmission. Finally, tables of space-time codes with good UEP capability are given by a computer search.

TABLE I
Good UEP STTC with QPSK Modulation and Two Transmit Antennas

	Memory	Generator Sequences	UEP Measurements
Low Diversity Case	2	$g_1 = [(3,2),(2,0)]$ $g_2 = [(1,0),(0,3)]$	$R(\boldsymbol{G}) = (2,2)$ $\Delta(\boldsymbol{G}) = (4,8)$
	3	$g_1 = [(2,2),(1,2)]$ $g_2 = [(2,0),(2,3),(2,1)]$	$R(\boldsymbol{G}) = (2,2)$ $\Delta(\boldsymbol{G}) = (8,16)$
	4	$g_1 = [(3,0),(1,1),(2,0)]$ $g_2 = [(1,2),(1,2),(0,2)]$	$R(\boldsymbol{G}) = (2,2)$ $\Delta(\boldsymbol{G}) = (12,16)$
	5	$g_1 = [(0,3),(1,1),(0,2)]$ $g_2 = [(0,2),(2,2),(1,1),(2,0)]$	$R(\boldsymbol{G}) = (2,2)$ $\Delta(\boldsymbol{G}) = (16,32)$
	6	$g_1 = [(1,1),(3,2),(3,0),(3,2)]$ $g_2 = [(2,0),(1,0),(3,2),(3,3)]$	$R(\boldsymbol{G}) = (2,2)$ $\Delta(\boldsymbol{G}) = (28,32)$
High Diversity Case	2	$g_1 = [(0,1),(1,0)]$ $g_2 = [(2,2),(0,2)]$	$R(\boldsymbol{G}) = (2,2)$ $\Omega(\boldsymbol{G}) = (4,12)$
	3	$g_1 = [(0,2),(0,3),(1,2)]$ $g_2 = [(2,0),(1,3)]$	$R(\boldsymbol{G}) = (2,2)$ $\Omega(\boldsymbol{G}) = (8,12)$
	4	$g_1 = [(3,1),(3,0),(0,1)]$ $g_2 = [(1,2),(2,1),(2,2)]$	$R(\boldsymbol{G}) = (2,2)$ $\Omega(\boldsymbol{G}) = (8,12)$
	5	$g_1 = [(0,3),(1,1),(0,3)]$ $g_2 = [(2,1),(3,2),(3,1),(2,3)]$	$R(\boldsymbol{G}) = (2,2)$ $\Omega(\boldsymbol{G}) = (8,14)$
	6	$g_1 = [(0,2),(0,1),(0,1),(1,1)]$ $g_2 = [(2,0),(3,1),(2,1),(3,1)]$	$R(\boldsymbol{G}) = (2,2)$ $\Omega(\boldsymbol{G}) = (12,16)$

References

[1] B. Masnick and J. K. Wolf, "On linear unequal error protection codes," *IEEE Trans. Inform. Theory*, vol. IT-13, pp. 600-607, July 1967.

[2] L. A. Dunning and W. E. Robbins, "Optimum encdoing of linear codes for unequal error protection," *Inform. Contr.*, vol. 37, pp. 150-177, 1978.

[3] R. Palazzo Jr., "Linear unequal error protection convolutional codes," in *Proc. 1985 IEEE Int. Symp. Inform. Theory*, Brighton, U.K., June 1985, pp. 88–89.

[4] M. C. Chiu, C. C. Chao, and C. H. Wang, "Convolutional codes for unequal error protection," in *Proc. IEEE Int. Symp. Inform. Theory*, Ulm, Germany, June 1997, p. 290.

[5] C. H. Wang and C. C. Chao, "Further results on unequal error protection of convolutional codes," in *Proc. IEEE Int. Symp. Inform. Theory*, Sorrento, Italy, June 2000, p. 35.

[6] V. Pavlushkov, R. Johannesson, and V. V. Zyablov, "Unequal error protection for convolutional codes," *IEEE Trans. Inform. Theory*, vol. 52, pp. 700–708, Feb. 2006.

[7] V. Tarokh, N. Seshadri, and A. R. Calderbank, "Space-time codes for high data rate wireless communication: performance criterion and code construction," *IEEE Trans. Inform. Theorey*, vol. 44, pp. 744-765, Mar. 1998.

[8] J. Yaun, Z. Chen, and B. Vucetic, "Performance and design of space-time coding in fading channels," *IEEE Trans. Commun.*, vol. 51, pp. 1991-1996, Dec. 2003.

[9] S. N. Diggavi, N. Al-Dhahir, and A. R. Calderbank, "Diversity-embedded space-time codes," in *Proc. IEEE GLOBECOM'03*, San Francisco, USA, Dec. 2003, pp. 1909-1914.

[10] C. Han and W. Wu, "UEP schemes for multimedia transmission in space-time coded systems," in *Proc. IEEE ICCCAS'07*, Fukuoka, Japan, July 2007, pp.602-606.

[11] C. H. Wang, T. M. Wu, L. D. Jeng, and C. W. Chen, "Rate-compatible punctured space-time codes for unequal error protection," in *Proc. IEEE VTC'04 (Fall)*, Los Angeles, USA, Sept. 2004, pp. 2379-2383.

[12] B. Abdool-Rassool, M. R. Heliot, F. Heliot, and H. Aghvami, "Concatenated space-time trellis codes with optimal puncturing patterns," *IEE Proc. Commun.*, vol. 152, no. 4, pp. 385-392, Aug. 2005.

[13] H. Jafarkhani and N. Seshadri, "Super-orthogonal space-time trellis codes," *IEEE Trans. Inform. Theory*, vol. 49, no. 4, pp. 937-950, April 2003.

[14] S. M. Alamouti, "A simple transmit diversity technique for wireless communications," *IEEE J. Sel. Areas Commun.*, vol. 16, no. 8, pp. 1451-1458, Oct. 1998.

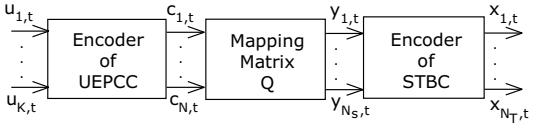

Fig. 3. The UEP scheme based on UEPCC-STBC.

TABLE II
UEP SPACE-TIME CODES BASED ON UEPCC-STBC
WITH QPSK MODULATION AND TWO TRANSMIT ANTENNAS

(N, K, V)	Generator Matrix	UEP Measurements
$(4, 2, 2)$	$\begin{pmatrix} 1 & 0 & 0 & 1 \\ 7 & 7 & 5 & 0 \end{pmatrix}$	$\Delta(\boldsymbol{G}) = (4, 144)$ $\Omega(\boldsymbol{G}) = (4, 24)$
$(4, 2, 3)$	$\begin{pmatrix} 1 & 1 & 0 & 0 \\ 13 & 0 & 15 & 17 \end{pmatrix}$	$\Delta(\boldsymbol{G}) = (64, 196)$ $\Omega(\boldsymbol{G}) = (16, 28)$
$(4, 2, 4)$	$\begin{pmatrix} 1 & 0 & 0 & 1 \\ 25 & 33 & 37 & 0 \end{pmatrix}$	$\Delta(\boldsymbol{G}) = (4, 256)$ $\Omega(\boldsymbol{G}) = (4, 32)$
$(4, 2, 5)$	$\begin{pmatrix} 1 & 0 & 7 & 6 \\ 14 & 13 & 15 & 5 \end{pmatrix}$	$\Delta(\boldsymbol{G}) = (144, 256)$ $\Omega(\boldsymbol{G}) = (24, 32)$
$(4, 2, 6)$	$\begin{pmatrix} 0 & 5 & 7 & 1 \\ 35 & 11 & 35 & 20 \end{pmatrix}$	$\Delta(\boldsymbol{G}) = (64, 256)$ $\Omega(\boldsymbol{G}) = (16, 32)$
$(4, 3, 2)$	$\begin{pmatrix} 0 & 0 & 1 & 1 \\ 1 & 0 & 1 & 0 \\ 5 & 7 & 0 & 0 \end{pmatrix}$	$\Delta(\boldsymbol{G}) = (4, 4, 64)$ $\Omega(\boldsymbol{G}) = (4, 4, 16)$
$(4, 3, 3)$	$\begin{pmatrix} 1 & 1 & 1 & 1 \\ 2 & 3 & 1 & 0 \\ 5 & 3 & 4 & 0 \end{pmatrix}$	$\Delta(\boldsymbol{G}) = (16, 36, 36)$ $\Omega(\boldsymbol{G}) = (8, 12, 12)$
$(4, 3, 4)$	$\begin{pmatrix} 1 & 1 & 1 & 1 \\ 1 & 2 & 3 & 0 \\ 16 & 5 & 15 & 0 \end{pmatrix}$	$\Delta(\boldsymbol{G}) = (16, 64, 100)$ $\Omega(\boldsymbol{G}) = (8, 16, 20)$
$(4, 3, 5)$	$\begin{pmatrix} 1 & 1 & 1 & 1 \\ 1 & 2 & 3 & 0 \\ 36 & 11 & 31 & 0 \end{pmatrix}$	$\Delta(\boldsymbol{G}) = (16, 64, 196)$ $\Omega(\boldsymbol{G}) = (8, 16, 28)$
$(4, 3, 6)$	$\begin{pmatrix} 1 & 1 & 1 & 1 \\ 3 & 1 & 2 & 0 \\ 57 & 40 & 21 & 0 \end{pmatrix}$	$\Delta(\boldsymbol{G}) = (16, 100, 144)$ $\Omega(\boldsymbol{G}) = (8, 20, 24)$
Mapping Matrix Q: $\begin{pmatrix} 2 & 0 & 0 & 1 \\ 0 & 2 & 1 & 0 \end{pmatrix}$		

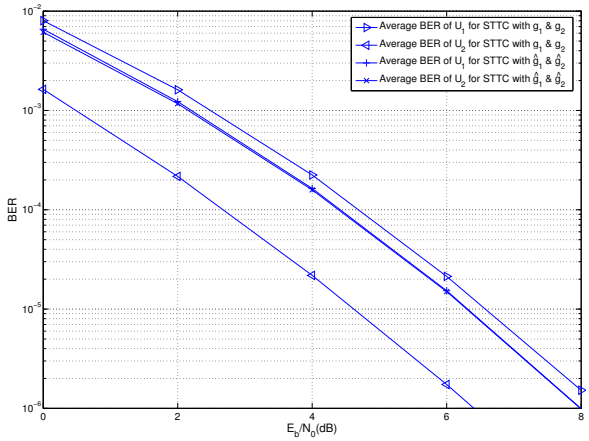

Fig. 1. Performance plots of STTC with generator sequences: $g_1 = [(0,1),(1,0)]$, $g_2 = [(2,0),(2,2)]$ and $\hat{g}_1 = [(0,1),(1,0)]$, $\hat{g}_2 = [(0,2),(2,0)]$, respectively.

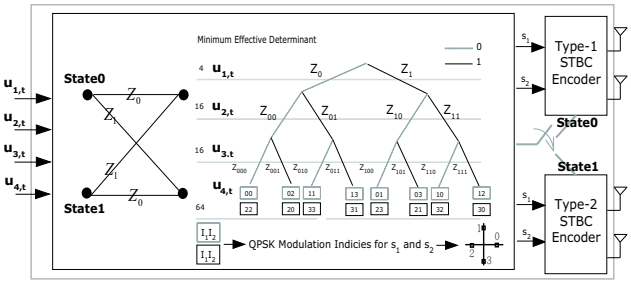

Fig. 2. The encoder structure of SOSTTC.

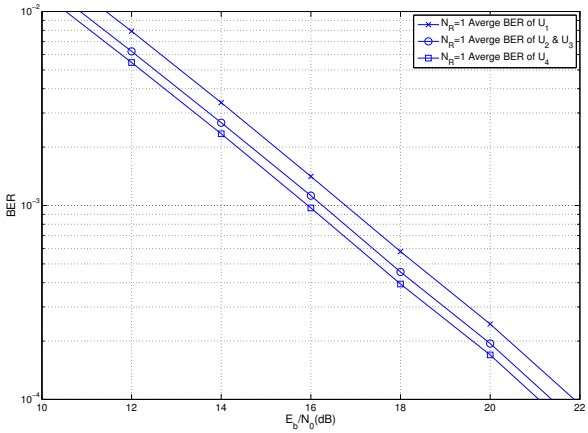

Fig. 4. Performance plots of SOSTTC with $N_T = 2$ and $N_R = 1$.

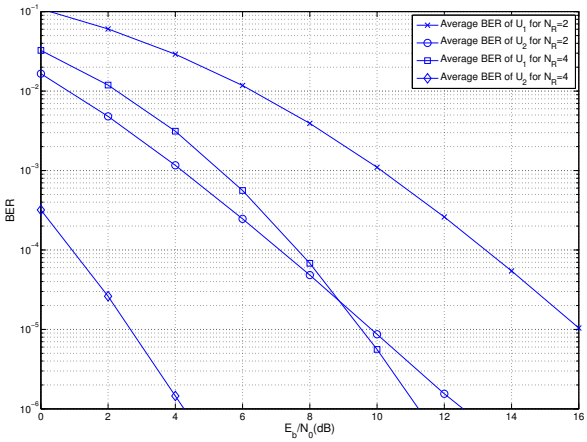

Fig. 5. Performance plots of UEPCC-STBC with two transmit antennas.

(a) Without UEP (b) With UEP

Fig. 6. The reconstructed images without and with UEP at SNR = -1dB.

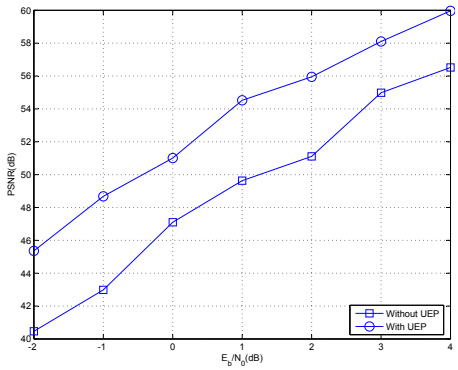

Fig. 7. PSNR curves of both reconstructed images for coding schemes with/without UEP.